



# Study on energy absorption characteristics of aluminum foam composite anti-collision rod

Chenghu Guo<sup>1</sup> · Jun Mao<sup>1</sup> · Miao Xie<sup>1</sup>

Received: 8 March 2022 / Accepted: 13 May 2022 / Published online: 6 June 2022  
© The Author(s), under exclusive licence to The Brazilian Society of Mechanical Sciences and Engineering 2022

## Abstract

Aiming at the poor energy absorption of anti-collision rod in automobile side door, a new anti-collision rod filled with foam aluminum composite structure is designed. Firstly, the mathematical model of aluminum foam composite structure is established, and the wall thickness and outer diameter of aluminum tube are taken as the critical factors. The influence of energy absorption effect is simulated and analyzed, and the correctness of the simulation is verified by experiments. Then, the filling rate of aluminum foam, the thickness of aluminum wall, the outer diameter of aluminum pipe and the number of energy absorption components are determined as four critical factors. The influence of four critical factors on the energy absorption effect of anti-collision rod is simulated and analyzed. Finally, the aluminum tube wall thickness, aluminum tube outer diameter and energy absorption components in the anti-collision rod are determined as critical independent variables, and the anti-collision rod is optimized by response surface optimization analysis method. The results show that compared with the traditional anti-collision rod, the optimized anti-collision rod improves the mass by 17% and the energy absorption by 80.27%. This study provides an important theoretical basis and experimental reference for vehicle energy absorption components in collision energy absorption.

**Keywords** Anti-collision rod · Aluminum foam composite structure · Response surface · Energy absorbing components · Optimized design

## 1 Introduction

With the number of cars increasing, more and more traffic accidents, especially side impact, and the injury rate is higher. People ensure the safety of people in the car by improving the crashworthiness of protective devices. Many automobile studies take the optimized automobile safety and crashworthiness as the primary tasks, so the research on automobile energy absorption components has certain practical significance and value [1].

When vehicle side impact occurs, the anti-collision rod is one of the main components to enhance vehicle crashworthiness. The research has proved that the automobile anti-collision rod has an irreplaceable role. Due to the narrow

space between the driver and the door, if there is no collision rod to absorb energy, it will produce great deformation and hurt the internal personnel [2].

Lightweight porous materials are combined with other structures to form composite structures, which absorb energy by plastic deformation and fracture [3]. Most commonly used are aluminum foam and honeycomb materials. Foam material is an ideal energy absorption material with small density, many voids, strong deformation ability and high total energy absorption during compression. However, there are many pores in the material itself and the strength is insufficient. When subjected to external force, it is easy to produce irreversible failure forms and lose integrity after failure [4]. Therefore, the average load of axial compression is increased when aluminum foam is filled into the metal tube, and the energy absorption effect of the composite structure is better than the sum of the energy absorbed by aluminum foam and thin-walled metal tube [5]. In the process of compression composite energy absorption components, the internal foam material will play a supporting role in the wall of thin-walled metal, so that the number of wrinkles increases. And the wall of thin-walled metal will also

---

Technical Editor: João Marciano Laredo dos Reis.

✉ Chenghu Guo  
1669733517@qq.com

<sup>1</sup> School of Mechanical Engineering, Liaoning Technical University, Fuxin 123000, China

have a reaction force on the foam material, so that it is fully squeezed, which will greatly improve the energy absorption of foam material [6].

In summary, aluminum foam has the advantages of small density, structural crashworthiness, strong energy absorption, shock absorption and noise reduction. Since its structure is porous material, it can achieve greater strength and stiffness with smaller mass. Combining it with hollow aluminum tube can not only reduce the disadvantages of using aluminum foam alone, but also increase the energy absorption. It has certain research value and significance to put such energy absorption device into the anti-collision rod to enhance the safety performance of the vehicle side [7].

### 2 Theoretical analysis of energy absorption characteristics of aluminum foam composite

As shown in Fig. 1, the energy absorption component of aluminum foam composite structure. According to the law of conservation of energy, the work done by the crushing force is equal to the sum of the energy generated by the rotation of the plastic hinge and the energy generated by the tension of the hollow aluminum tube wall [8].

As shown in Fig. 2, when the rotation angle of plastic hinge is  $da$ , the generated energy:

$$dE_1 = 4\pi M_0(2r + h \sin \alpha)d\alpha \tag{1}$$

where  $dE_1$  is the energy produced by the rotation of plastic hinge;  $\delta_0$  is the yield limit of hollow aluminum tube;  $r$  is the inner radius of hollow aluminum tube;  $h$  is the half wavelength of wrinkle;  $\alpha$  is the angle of thin-walled rotation of hollow aluminum tube;  $M_0$  is the bending moment limit of hollow aluminum tube.

Energy generated by thin-walled tension of hollow aluminum tube [9]:

$$dE_2 = 2\pi\delta_0 h^2 t \cos \alpha d\alpha \tag{2}$$

The load of hollow aluminum tube under quasi-static crushing:

Fig. 1 Aluminum foam composite structure

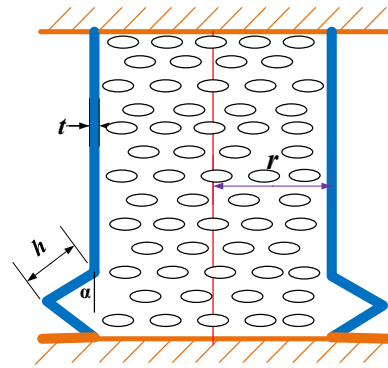


Fig. 2 Crush model of composite structure

$$P_c = \left( \frac{1}{2}\pi t^2 + \pi t\sqrt{2\pi r t} \right) \delta_0 \tag{3}$$

The contribution of interaction between aluminum foam and hollow aluminum tube wall to crushing load:

$$\Delta l = C_{avg} \times \delta_f^{a_1} \times \delta_0^{a_2} \times r^{a_3} \times t^{a_4} \tag{4}$$

where  $\delta_f$  is yield limit of aluminum foam;  $C_{avg}$ ,  $a_1$ ,  $a_2$ ,  $a_3$ ,  $a_4$  are constants. By sorting out:

$$\Delta l = 2.5\sqrt{\delta_f \delta_0} (rt) \tag{5}$$

Axial crushing load produced by compression of aluminum foam in aluminum tubes:

$$P_f = \pi r^2 \delta_f \tag{6}$$

$$\frac{\delta_f}{\delta_s} = 0.3\phi(\rho')^{\frac{3}{2}} + (1 - \phi)\rho' \tag{7}$$

where  $\delta_s$  is yield Limit of Foamed Aluminum.  $\phi$  is the content of material between small element thin walls in aluminum foam.

$$\rho' = \rho_f / \rho_s \tag{8}$$

where  $\rho_f$  is the density of aluminum foam;  $\rho_s$  is the density of solid materials that make up aluminum foam.

$$\delta_f = \rho' \delta_s \tag{9}$$

Load of Aluminum Foam Composite Structure under Quasi-static Compression:

$$P_k = P_c + P_f + \Delta l = \left[ \frac{1}{2}\pi t^2 + \pi t\sqrt{2\pi r t} \right] \delta_0 + \pi r^2 \rho' \delta_s + 2.5\sqrt{\delta_f \delta_0} (rt) \tag{10}$$

Energy absorption of hollow aluminum tube under quasi-static crushing:

$$W_k = P_c l \xi_c = \left( \frac{1}{2} \pi t^2 + \pi t \sqrt{2\pi r t} \right) \delta_0 l \xi_c \tag{11}$$

where  $l$  is length of hollow aluminum tube;  $\xi_c$  is compression strain of hollow aluminum tube.

Energy Absorption of Aluminum Foam Composite Structure under Quasi—static Compression:

$$W_F = P_k l \zeta_D = (P_c + P_f + \Delta l) l \zeta_D = \left[ \frac{1}{2} \pi t^2 + \pi t \sqrt{2\pi r t} \right] \delta_0 + \pi r^2 \rho' \delta_s + 2.5 \sqrt{\delta_f \delta_0} (r t) \tag{12}$$

where  $\rho'$  is relative density of aluminum foam;  $\zeta_D$  is Compression strain of aluminum foam composite structure.

Compressive strain of aluminum foam during crushing:

$$\zeta_f = 1 - 1.4 \frac{\rho_f}{\rho_s} = 1 - 1.4 \rho' \tag{13}$$

The compaction strain of hollow aluminum tube:

$$\xi_c = 1 - \frac{t}{h} = 1 - \sqrt{\frac{2t}{\pi r}} \tag{14}$$

Compaction strain of aluminum foam composite structure:

$$\zeta_D = \min(\zeta_f, \xi_c) \tag{15}$$

Composite is the energy absorption of aluminum foam composite structure under quasi-static crushing

$$W_F = \min(1 - \sqrt{2t/r}, 1 - 1.4\rho') \times \left[ \frac{1}{2} \pi t(t + 2\sqrt{2\pi r t}) \delta_0 + \pi r^2 \rho' \delta_s + 2.5 r t \sqrt{\rho' \delta_0 \delta_s} \right] \times l \tag{16}$$

As shown in Fig. 3, the yield limit of hollow aluminum tube:

$$\delta_0^d = \delta_0 \left[ 1 + \left( \frac{\dot{\zeta}}{\mu} \right)^{\frac{1}{n}} \right] \tag{17}$$

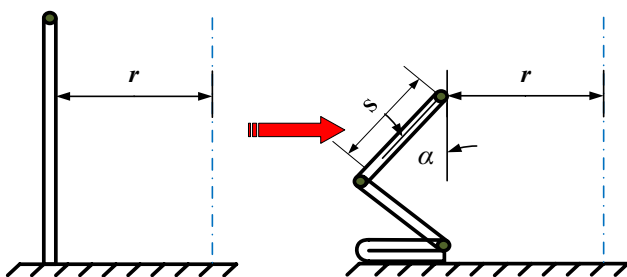


Fig. 3 Aluminum tube break element

where  $\delta_0^d$  is the yield limit of hollow aluminum tube under dynamic condition.  $\dot{\zeta}$  is strain rate for hollow aluminum tubes.  $\mu, n$  is the strain rate sensitivity coefficient. The load of hollow aluminum tube under dynamic crushing:

$$P_c^d = P_c \left[ 1 + \left( \frac{\dot{\zeta}}{\mu} \right)^{\frac{1}{n}} \right] \tag{18}$$

The load of hollow aluminum tube under dynamic crushing:

$$P_c^d = P_c \left[ 1 + \left( \frac{V_0}{4r\mu} \right)^{\frac{1}{n}} \right] = \left[ \frac{1}{2} \pi t^2 + \pi t \sqrt{2\pi r t} \right] \delta_0 \left[ 1 + \left( \frac{V_0}{4r\mu} \right)^{\frac{1}{n}} \right] \tag{19}$$

Axial crushing load:

$$P_f = \pi r^2 \delta_f \tag{20}$$

Yield Limit of Built-in Aluminum Foam under Dynamic Compression

$$\delta_f^d = \delta_f^0 \left( \frac{\dot{\zeta}_f}{\dot{\zeta}_f^0} \right)^m \tag{21}$$

where  $\delta_f^0$  is strain rate under dynamic crushing;  $\dot{\zeta}_f$  is strain of Aluminum Foam.

The ultimate load expression of aluminum foam composite structure in dynamic crushing process

$$P_k^d = P_c^d + P_f^d + \Delta l = \left[ \frac{1}{2} \pi r^2 + \pi t \sqrt{2\pi r t} \right] \delta_0 \left[ 1 + \left( \frac{V_0}{4r\mu} \right)^{\frac{1}{n}} \right] + \pi r^2 \delta_f \left( \frac{V_0}{2l\dot{\zeta}_f^0} \right)^m + \Delta l \tag{22}$$

where  $P_k^d$  is The crushing load of aluminum foam composite structure under dynamic compression;  $P_c^d$  is the crushing load of hollow aluminum tube under dynamic compression;  $P_f^d$  is the crushing load of aluminum foam during dynamic compression;  $\Delta l$  is the interaction between aluminum foam and hollow aluminum tube wall;  $\dot{\zeta}_f^0$  is the strain rate of aluminum foam in quasi-static crushing process;  $m$  is the strain rate sensitivity coefficient.

Energy of hollow aluminum tube during dynamic crushing:

$$W_k^d = P_c^d l \xi_c = \left[ \frac{1}{2} \pi t^2 + \pi t \sqrt{2\pi r t} \right] \delta_0 \left[ 1 + \left( \frac{V_0}{4r\mu} \right)^{\frac{1}{n}} \right] l \xi_c \tag{23}$$

where  $W_k^d$  is energy absorption of hollow aluminum tubes during dynamic crushing;  $\zeta_c$  is the compression strain of the hollow aluminum tube.

Energy of Aluminum Foam Composite Structure in Dynamic Crushing Process:

$$W_F^d = \zeta_D (P_k^d + P_c^d + \Delta l) l = \min \left( 1 - \sqrt{\frac{2t}{r\pi}}, 1 - 1.4\rho' \right) \cdot \left\{ \left( \frac{1}{2}\pi t^2 + \pi t\sqrt{2\pi r t} \right) \delta_0 \left[ 1 + \left( \frac{V_0}{4r\mu} \right)^{\frac{1}{n}} \right] + \pi r^2 \rho' \delta_s \left( \frac{V_0}{2l\zeta_f^0} \right)^m + 2.5rt\sqrt{\rho' \delta_0 \delta_s} \right\} \cdot l \tag{24}$$

### 3 Energy absorption characteristics analysis of aluminum foam composite members

#### 3.1 Evaluation index of energy absorption characteristics of energy absorption components

1. Total energy [10]  
The total absorbed energy represents the energy absorbed during the deformation of the component during the whole collision process.
2. Peak force [11]  
Peak force represents the maximum impact force during collision.
3. Average impact force.  
The arithmetic average of the collision force curve on the whole compression displacement  $s$  during the whole collision process.

$$F_m = \frac{E}{s} \tag{25}$$

4. Specific energy absorption [12]  
Specific energy absorption represents the energy that the component can absorb per element mass in the whole collision process.

$$E_{SA} = \frac{E}{m} \tag{26}$$

5. Compression efficiency.  
Compression efficiency is the ratio of average load to peak loads

$$E_{CF} = \frac{F_m}{F} \tag{27}$$

#### 3.2 Parameters of new anti-collision bar

According to the size of the anti-collision bar of a certain type of automobile, the size of the new anti-collision bar is obtained, as shown in Table 1. Figure 4 introduces the main composition of the anti-collision bar.

The size range of the foam aluminum composite component in the new bumper rod is shown in Table 2.

The material properties of the new anti-collision bar are shown in Table 3.

#### 3.3 Analysis of energy absorption characteristics of aluminum foam composite structure

Hollow aluminum pipe is selected, with outer diameter  $D=30$  mm, height  $H=30$  mm, thickness  $t=1$  mm. Choose foam aluminum composite structure, outer diameter  $D=30$  mm, height  $H=30$  mm.

The collapse simulation analysis of the hollow aluminum tube and aluminum foam composite structure is carried out by ANSYS. The model is shown in Fig. 5a and b. It consists of two upper and lower rigid plates and a foam aluminum composite structure. The lower rigid plate is fixed and the upper rigid plate is axially compressed. The contact surface is between the foam aluminum and the hollow tube, and the friction coefficient between the two rigid plates and the hollow aluminum tubes is 0.2.

To verify the foam aluminum composite structure in the simulation analysis process, the energy absorption characteristic curve is accurate. Test the mechanical properties of the sample on the testing machine, as shown in Fig. 6. The foam aluminum composite structure is made up of aluminum foam and hollow aluminum tube. When doing the experiment, the aluminum foam is placed in the hollow aluminum tube, and the surface is not bonded. The test piece is placed at the center of the lower end of the bottom plate of the testing machine, the upper steel plate moves downward evenly, and the loading speed is 3 mm/min.

Under the same external conditions, the displacement force characteristic curve of hollow aluminum tube in simulation and experiment is obtained, as shown in Fig. 7; Under the same applied conditions, the displacement force characteristic curves of the aluminum foam composite structure in simulation and experiment are obtained, as shown in Fig. 8. By analyzing the curves in Figs. 7 and 8, it is found that the overall trend and fluctuation of the curve are similar [13].

**Table 1** Dimensions of anti-collision bar

Length/mm	Wide/mm	High/mm	Wall thickness/mm
959	32	32	2

**Fig. 4** Structural composition of new anti-collision bar

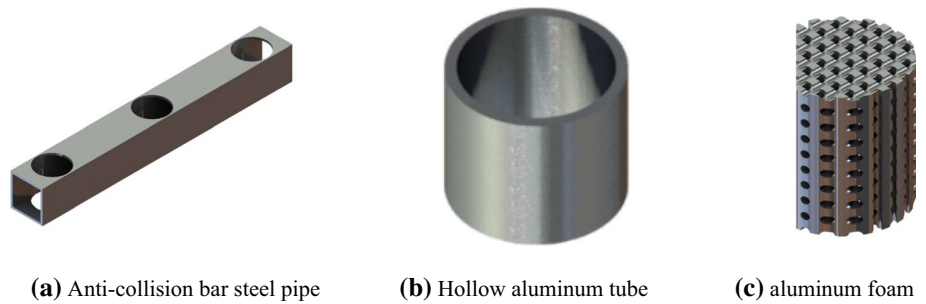


**Table 2** Dimensions of energy absorbing components

Outer diameter/mm	Wall thickness/mm	$n$	Length/mm	Arrangement style
$18 \leq D \leq 30$	$0 < t \leq 6$	$n \leq 17$	30 mm	Uniform distribution

**Table 3** Material properties of new anti-collision bar

Name	Material	Elastic modulus	Poisson's ratio	Density/ $\text{kg}\cdot\text{mm}^{-3}$
anti-collision bar	Q235	201Gpa	0.3	7850
Aluminum tube	Al 6061-T6	68.9Gpa	0.33	2703
Aluminum foam	Al	253Mpa	0.33	178

To visually express the error between the simulation results and the test results, the error percentage histogram is drawn, as shown in Fig. 9. The maximum error of test and simulation data of hollow aluminum tube is 15.86%, and the minimum error is 1.8%. The maximum error of test and simulation data of foam aluminum composite structure is 24.21% and the minimum is 4.68%. The simulation results are consistent with the experimental results, and the fluctuation trend is similar. Therefore, the simulation results are reliable.

**Fig. 5** Simulation model of energy absorbing component

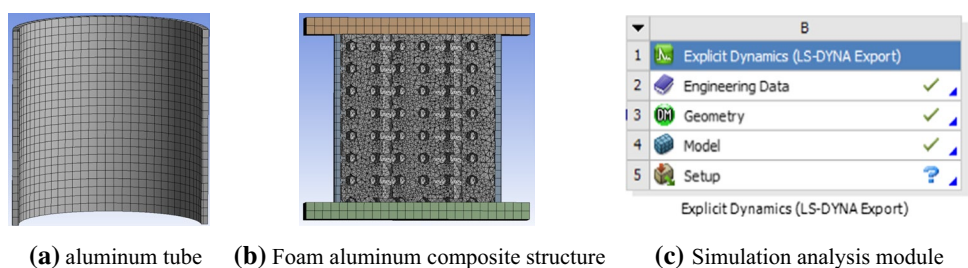


**Fig. 6** Foam aluminum composite structure on test machine

### 3.4 Parametric experimental analysis of energy absorption characteristics of aluminum foam composite structure

The outer diameter of aluminum foam composite structure is  $D=30$  mm, the height  $H=30$  mm, and the thickness of hollow aluminum tube is  $t=1, 1.6, 2.2$ . The static crushing test is carried out, and the load displacement characteristic curve is obtained [14].

As shown in Fig. 10, after the compression of the aluminum foam composite structure, an outwardly folded axisymmetric fold is generated. First, the load of aluminum foam composite structure increases continuously during axial compression. After reaching the first peak force, it begins to show a downward trend and enter the buckling stage. Finally, the curve rises sharply and enters the compaction stage. The whole process produces only one wave, so the deformation presents only one wrinkle. As can be

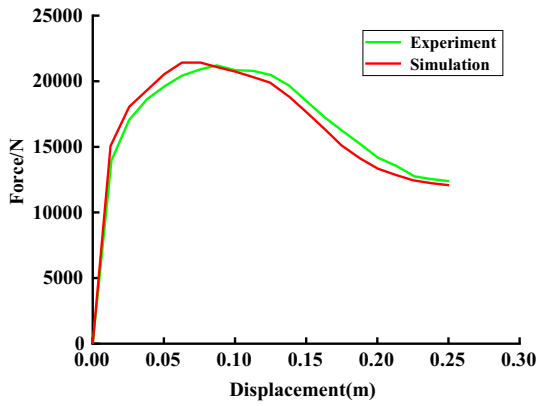


Fig. 7 Energy absorption curve of aluminum tube

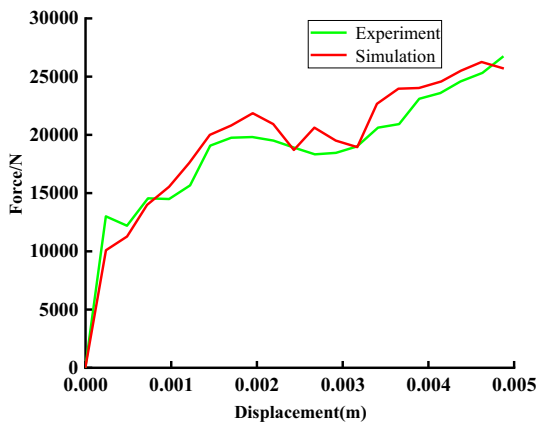
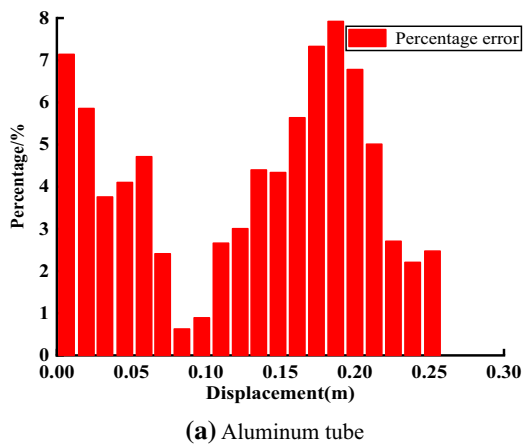


Fig. 8 Energy absorbing curve of foam aluminum composite structure



seen from Fig. 10, as the wall thickness increases, the corresponding compressive load increases. It shows that the load-carrying capacity of the aluminum foam composite structure is increasing, and the wall thickness can absorb more energy. However, while increasing the energy absorption, it is necessary to ensure the design requirements of strong quantification of components.

The wall thickness  $t = 1$  mm, the height  $H = 30$  mm, the outer diameter of hollow aluminum tube is  $D = 26, 28, 30$  mm. The static crushing experiment was carried out and the load–displacement curve was obtained.

It can be seen from Fig. 11 that after compression, the foam aluminum composite structure generates an axisymmetric wrinkle that folds outward. From the curve, the larger the diameter, the greater the peak force. The aluminum foam composite structure with large diameter is filled with more aluminum foam. During the compression process, the aluminum foam structure collapses, ruptures, and compacts. The mutual constraints between each small gap and between aluminum foam and hollow aluminum tubes will absorb more energy.

#### 4 Parameterized analysis of energy absorption characteristics of the new anti-collision rod

The new anti-collision rod is composed of hollow square tube, aluminum foam and aluminum tube. Through the single factor research method [14, 15], the filling rate of aluminum foam, the outer diameter and wall thickness of hollow aluminum tube and the number of energy absorption components in the anti-collision rod are taken as the key factors, and the parametric simulation analysis is carried out. The simulation model is shown in Fig. 12.

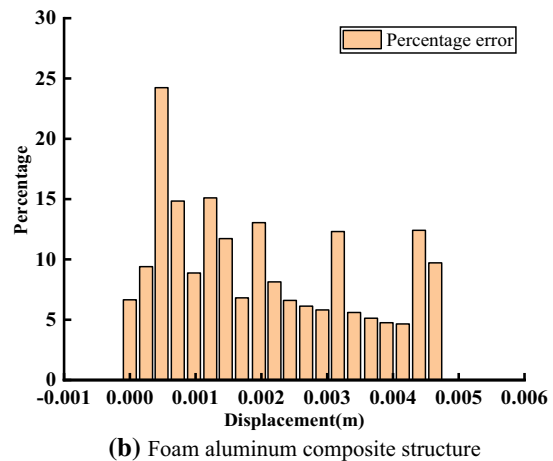
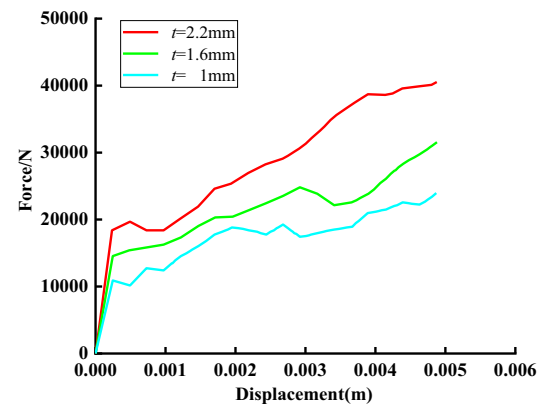
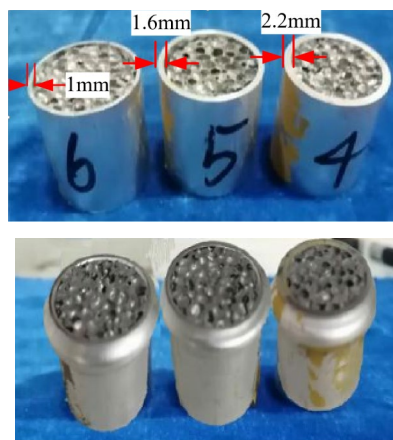


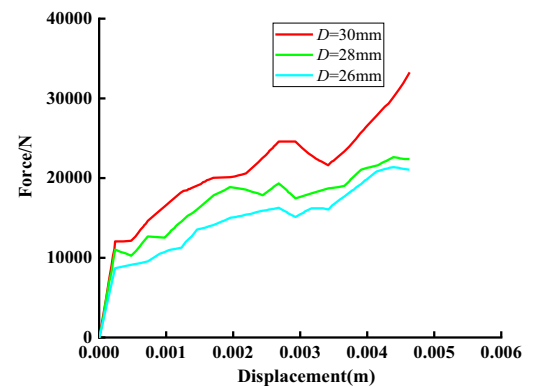
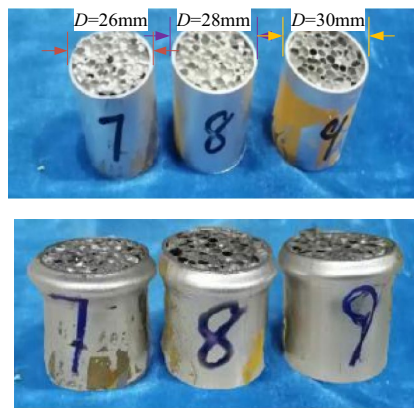
Fig. 9 Histogram of error percentage of energy absorbing components



**Fig. 10** Compression test of aluminum foam composite structure (wall thickness comparison)



**Fig. 11** Compression test of aluminum foam composite structure (comparative diameter)



The cylindrical rigid body is compressed at 8.3 m/s along the axis of the composite structure. Fix both ends of the anti-collision bar, and fix the energy absorbing member on the inner surface of the anti-collision bar. The contact surface is between the foam aluminum composite structure and the hollow square tube. The friction coefficient between the cylindrical rigid body and the hollow square tube is 0.2, and the general contact is adopted [16–19].

#### 4.1 Effect of filling percentage on energy absorbing components of impact bar under dynamic crushing

To reduce the usage of foam aluminum, the influence of percentage of filled aluminum foam on energy absorption index was studied. The energy absorbing component is  $H=30$  mm height, wall thickness  $t=1$  mm and outer diameter  $D=30$  mm. Four kinds of foam aluminum composite structure filled with 0, 25%, 50%, 75% and 100% percentages are designed. The three-dimensional model of energy absorbing component is shown in Fig. 13.

According to the analysis of Fig. 14, the hollow aluminum tube is filled with 25%, 50%, and 75% aluminum foam. Due to the interaction between aluminum foam and hollow aluminum tube, the component does not undergo axisymmetric deformation. There is a coupling effect between aluminum foam and aluminum tube, resulting in random and extremely unstable deformation process. With the increase of aluminum foam filling percentage, the deformation morphology of energy absorption components is more and more stable. From the load–displacement curve, the compression displacement is the same, the filling percentage is more, the peak force is larger, and the absorbed energy is more. From

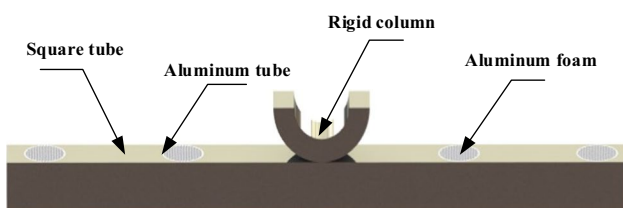


**Fig. 12** New anti-collision bar

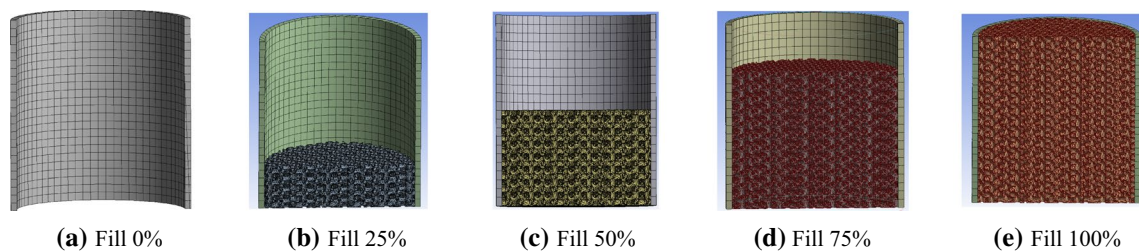


Fig. 13 Energy absorbing member

Fig. 14 Crushing curve of energy absorbing member under different filling percentage

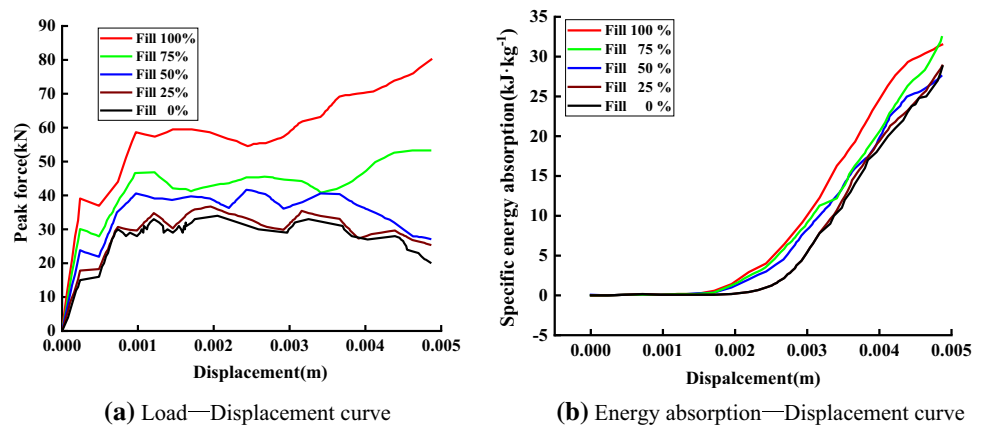


Table 4 Energy absorption indexes of energy absorbing components under different filling percentages

	Peak force/kN	Energy/kJ	Quality/kg	Specific energy absorption/ kJ kg <sup>-1</sup>
Fill 0%	30.69	23.86	0.9544	25.37
Fill 25%	32.28	28.71	0.9582	29.96
Fill 50%	37.45	32.56	0.9632	33.81
Fill 75%	53.84	26.03	0.9682	26.88
Fill 100%	76.42	33.61	0.9732	34.54

Table 4, it is concluded that the energy absorption effect of filling 50% is the best in terms of energy and specific energy absorption, but the unstable deformation does not meet the design requirements. The peak force and energy of 100% filling are the largest, and the specific energy absorption per unit mass is also the largest. Therefore, 100% filling method is selected as the research object.

### 4.2 Effect of outer diameter under dynamic crushing on energy absorption characteristics of anti-collision bar

To study the influence of the outer diameter of the hollow aluminum tube on the energy absorption characteristics of

the new anti-collision rod, the aluminum wall thickness  $t = 1$ , the height  $H = 30$  mm, and the outer diameter of the aluminum tube  $D = 22, 24, 26, 28$  and 30 mm were designed. The influence of the outer diameter of the aluminum tube on the energy absorption characteristics of the new anti-collision rod was simulated and analyzed.

As shown in Fig. 15a, it conclude that the new anti-collision rod tends to increase gradually after reaching the initial peak load. During the compression process, there will be wrinkles in the aluminum tube, and aluminum foam will restrict and interact with the aluminum tube. As shown in Fig. 15b and c, the specific energy absorption tends to increase with the increase of outer diameter. As shown in Table 5, with the increase of outer diameter, peak force, energy absorption and mass are increasing, and its specific energy absorption is also increasing. Overall, the bearing capacity of the anti-collision rod increases with the increase of the outer diameter of the hollow aluminum tube. The external diameter increases, the mass of aluminum foam filled inside increases, and the absorbed energy increases. However, the larger the outer diameter is, the larger the space will be occupied. Therefore, according to the actual working conditions, the appropriate outer diameter of hollow aluminum tube should be selected to ensure that there is enough space to install energy absorption components and absorb more energy.



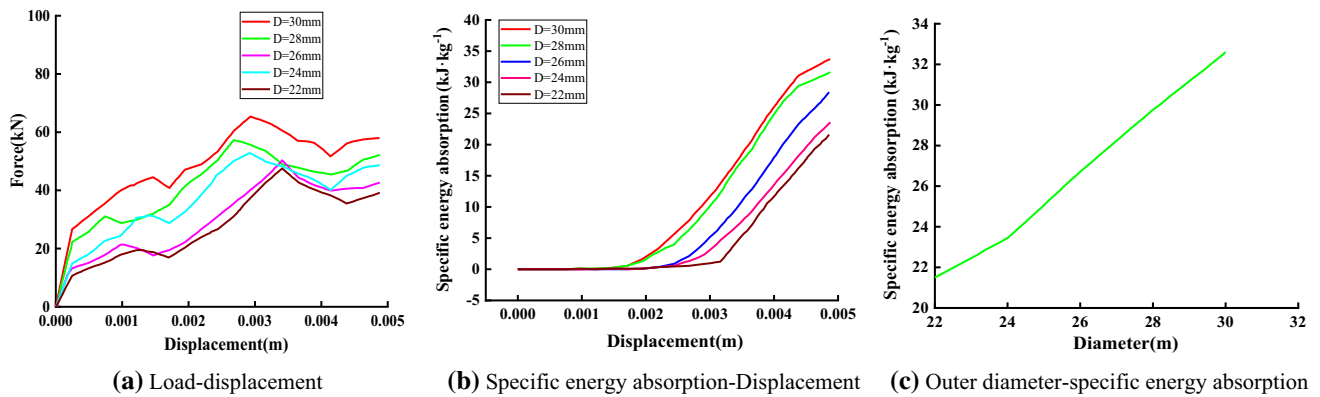


Fig. 15 Dynamic crushing curves of energy absorbing members with different outer diameters

Table 5 Energy absorption indexes of energy absorbing components with different outer diameters

	Peak force/kN	Energy/kJ	Quality/kg	Specific energy absorption/ kJ kg <sup>-1</sup>
D=22 mm	53.54	19.84	0.9215	21.54
D=24 mm	56.53	21.94	0.9354	23.45
D=26 mm	61.64	25.20	0.9428	26.73
D=28 mm	64.55	28.37	0.9534	29.76
D=30 mm	73.46	31.36	0.9625	32.58

### 4.3 Effect of wall thickness on energy absorption characteristics of anti-collision bar under dynamic crushing

To study the influence of hollow aluminum tube diameter on the energy absorption characteristics of new anti-collision rod, the aluminum tube diameter  $D = 30$  mm, height  $H = 30$  mm, aluminum wall thickness  $t = 1, 1.6, 2.2, 2.7$  and  $3.2$  mm of foam aluminum composite energy absorption

component were designed. The influence of aluminum tube diameter on the energy absorption characteristics of new anti-collision rod was simulated and analyzed.

As shown in Fig. 16, the specific energy absorption of the anti-collision rod increases with the increase of the wall thickness of the internal aluminum foam composite energy absorption member, but the increasing process slowly tends to be flat. It is proved that the wall thickness of the energy absorption member inside the anti-collision rod becomes thinner, and the more foam aluminum is filled, the greater the rigid-flexible coupling effect between the foam aluminum and the wall is. As shown in Table 6, it conclude that at the same compression displacement, its peak force, energy absorption and specific energy absorption are increasing with the increase of wall thickness. Overall, the bearing capacity of anti-collision rod increases with the increase of hollow aluminum tube wall thickness. But the greater the wall thickness, the quality of aluminum pipe will increase, so should be based on the actual working conditions, consider choosing the appropriate thickness, while ensuring lightweight, absorb more energy.

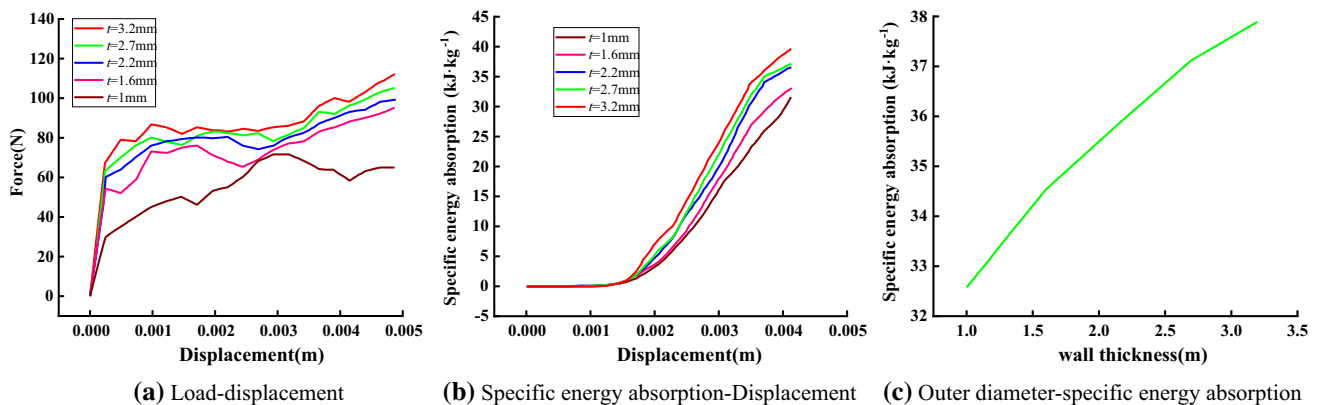


Fig. 16 dynamic crushing curve of energy absorbing members with different wall thickness

**Table 6** energy absorption indexes of energy absorbing components with different wall thickness

	Peak force/kN	Energy/kJ	Quality/kg	Specific energy absorption/ kJ kg <sup>-1</sup>
<i>t</i> = 1 mm	73.46	31.36	0.9625	32.58
<i>t</i> = 1.6 mm	76.42	33.61	0.9732	34.54
<i>t</i> = 2.2 mm	80.25	35.42	0.9876	35.86
<i>t</i> = 2.7 mm	83.14	36.92	0.9945	37.12
<i>t</i> = 3.2 mm	86.47	42.63	1.1253	37.89

**Table 7** energy absorption indexes of different number of energy absorbing components

	Peak force/kN	Energy/kJ	Quality/kg	Specific energy absorption/ kJ kg <sup>-1</sup>
<i>n</i> = 5	107.86	47.89	1.1342	42.23
<i>n</i> = 6	114.37	53.74	1.1744	45.76
<i>n</i> = 7	120.52	59.41	1.2147	48.91
<i>n</i> = 8	123.74	63.29	1.2549	50.44
<i>n</i> = 9	127.46	66.37	1.2952	51.24

#### 4.4 Effect of the number of energy absorbing members on the energy absorption characteristics of anti-collision bar under dynamic crushing

The energy absorbing members are placed on the inner side of the hollow steel pipe and arranged with 5, 6, 7, 8 and 9 respectively. Ensure that the outer diameter and wall thickness of other variables of the energy absorbing member remain unchanged. Analyzing the influence of a single variable on the energy absorbing characteristics of the anti-collision rod.

As shown in Fig. 17a, with the increase of the number of energy absorbing components in the new anti-collision rod, the peak force increases under the same compression displacement. As shown in Fig. 17b and Table 7, with the increase of the number of elements, its peak force, energy and mass are increasing at the same compression displacement. It is proved that in a certain range, with the increase of the number of energy absorbing components, the energy absorbing characteristics of the anti-collision bar are obviously enhanced. However, with the increase in the number of energy absorption components, the strength of the hollow square tube will decrease. Therefore, it is necessary to analyze the number of energy absorption components according

to the actual working conditions, absorbing more energy while ensuring the strength of the square tube.

### 5 Influence Analysis and optimization of multi factor structural parameters on energy absorbing components of anti-collision bar

The influence of the three factors on the energy absorption characteristics of the bumper rod is studied by studying the outer diameter of the aluminum composite component, the thickness of the aluminum tube and the number of energy absorbing members [20–22].

#### 5.1 Dynamic collision analysis of anti-collision bar under multiple factors

Since the objective function is a nonlinear programming problem, a constraint condition is added to draw the response surface of the fitting curve, which belongs to the constrained optimization problem. Limit *n*, *t* and *D* respectively through the control variable method, and observe the influence of the other two variables on energy absorption, as shown in Figs. 18, 19 and 20.

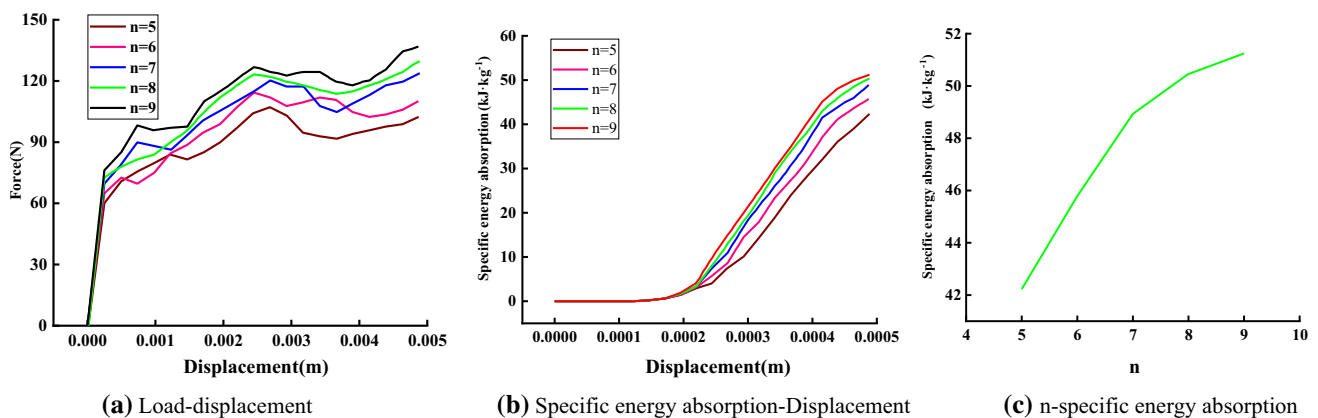


**Fig. 17** dynamic crushing curve of energy absorbing members with different wall thickness

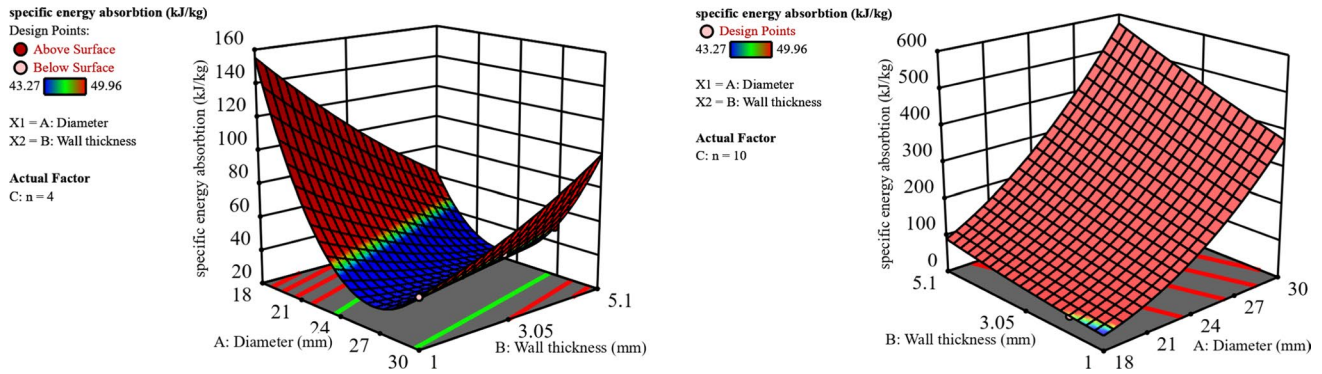


Fig. 18 Response surface of specific energy absorption with respect to outer diameter and wall thickness

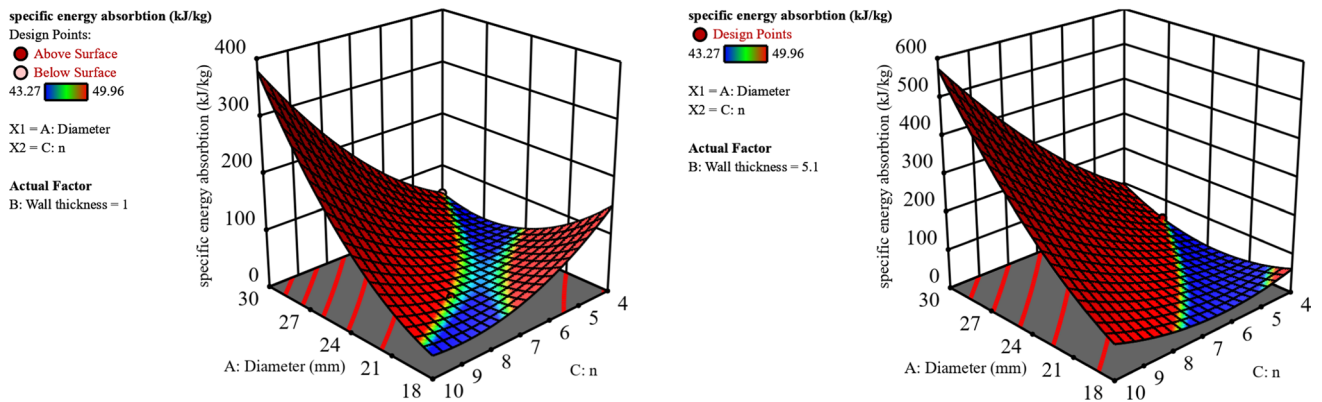


Fig. 19 Response curve of specific energy absorption with respect to outer diameter and number of energy absorbing members

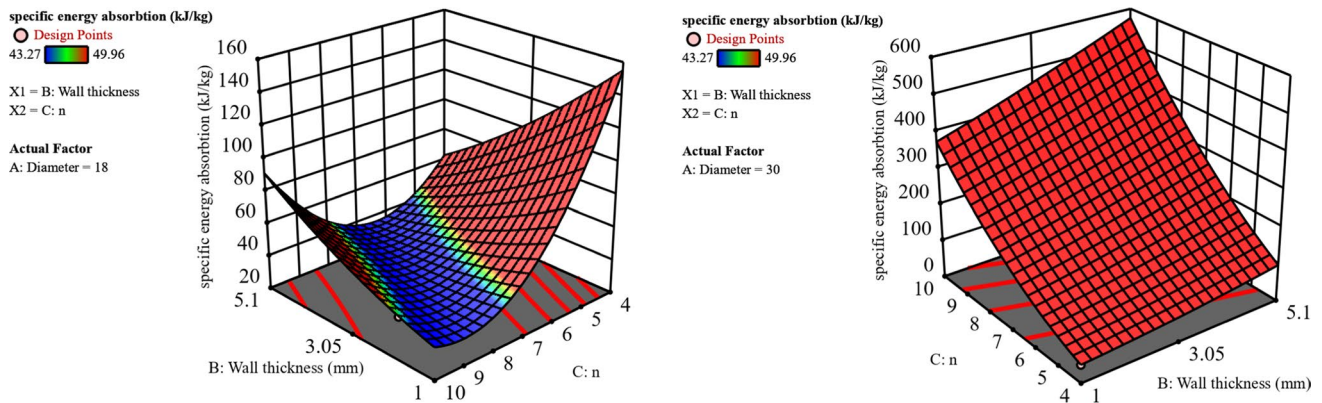


Fig. 20 Response curve of specific energy absorption with respect to wall thickness and number of energy absorbing members

### 5.2 Optimization of energy absorbing components of anti-collision bar.

To meet the optimal energy absorption and ensure the lightness of the vehicle. The outer diameter, wall thickness and

the number of energy absorbing components need to be optimized. The specific energy absorption is selected as the objective function. According to the data in Table 8, the optimal fitting curve is calculated:

**Table 8** various schemes of energy absorbing components of anti-collision bar

<i>D</i> /mm	<i>t</i> /mm	<i>n</i>	Peak force /kN	Energy/kJ	Quality /kg	Specific energy absorption/ kJ kg <sup>-1</sup>
30	1	4	122.14	53.78	1.094	49.16
29	2.2	4	118.94	53.14	1.094	48.58
28	3.5	4	114.59	52.07	1.094	47.60
27	5.1	4	110.04	51.37	1.094	49.96
27	1	5	113.59	51.62	1.094	47.19
26	1.8	5	104.87	49.48	1.094	45.23
25	3.2	5	100.43	48.29	1.094	44.14
24	1.4	6	109.45	51.23	1.094	46.83
24	4.9	5	95.72	47.34	1.094	43.27
23	2.7	6	105.13	49.96	1.094	45.67
22	1.6	7	113.67	51.61	1.094	47.18
22	4.3	6	101.24	48.49	1.094	44.33
21	1	8	117.45	52.69	1.094	48.16
21	3.2	7	114.21	52.00	1.094	47.53
20	2.2	8	101.36	48.38	1.094	44.23
20	4.7	7	118.43	53.88	1.094	49.25
19	1.85	9	117.35	52.78	1.094	48.25
19	3.8	8	113.83	51.83	1.094	47.38
18	1.8	10	109.17	50.56	1.094	46.22
18	3.4	9	113.54	51.68	1.094	47.24

$$Y = 1327.3 - 781.2D - 659.4t - 138.3n + 186.6Dt + 39.2tn + 82.5Dn + 224.8D^2 + 63.6t^2 + 3n^2 \tag{28}$$

The outer diameter, wall thickness and number of energy-absorbing components of the anti-collision bar must meet the design size range, and these three variables must meet the requirement that the increased mass of the anti-collision bar shall not exceed 20%.

$$\begin{cases} 18 \text{ mm} \leq D \leq 30 \text{ mm} \\ 1 \text{ mm} \leq t \leq 6 \text{ mm} \\ n \leq 17 \\ M_{new} = \left\{ \rho_1 \pi H \left( \frac{D}{2} - t \right)^2 + \rho_2 \pi H \left[ \frac{D^2}{4} - \left( \frac{D}{2} - t \right)^2 \right] \right\} n \end{cases} \tag{29}$$

Through analysis, when  $n=8$ ,  $D=21$  mm and  $t=1$  mm, the specific energy absorption value is the largest and is the optimal solution. As shown in Fig. 21.

The energy absorption characteristics of the optimized anti-collision bar are simulated and analyzed, and compared with the traditional anti-collision bar. As shown in the Fig. 22.

The new anti-collision rod is composed of a hollow square tube and a foam aluminum composite structure. In the process of collision, the hollow square tube will produce elastic and plastic deformation. In addition to the elastic and

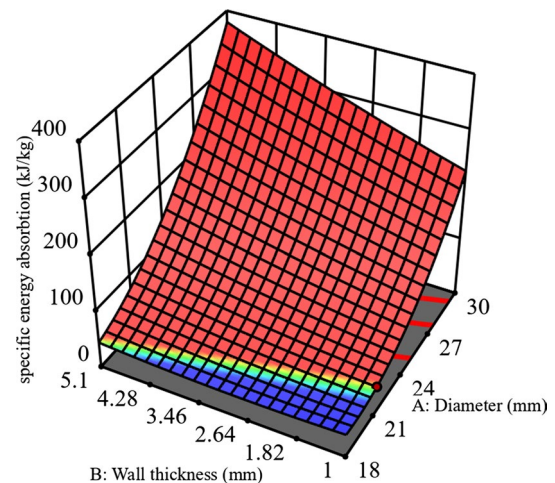


**Fig. 21** Optimal solution of specific energy absorption

plastic deformation of aluminum foam composite devices, aluminum foam will absorb a lot of energy in the process of compaction. At the same time, there will be some wrinkles between the aluminum foam composite structure and the aluminum foam composite structure. The folds will support each other and restrict each other, which will greatly improve the peak force and energy absorption. From Fig. 22a and b, it is concluded that the collision load of the anti-collision rod containing aluminum foam composite structure is 126.67 kN



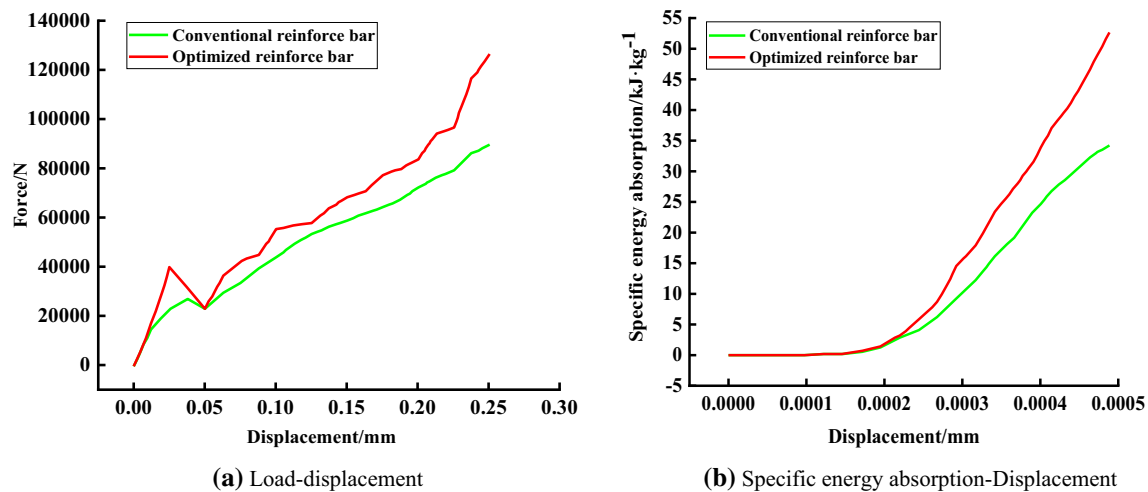


**Fig. 22** Dynamic energy absorption characteristic curves of different anti-collision bars

and the energy is 57.56 kJ. The impact load of traditional anti-collision bar is 89.49kN and the energy absorption is 31.93 kJ. The load is increased by 41.55%, the energy absorption is increased by 80.27%, and the energy absorption is greatly improved. Therefore, the new anti-collision rod containing aluminum foam composite structure can meet the development requirement of the car.

## 6 Conclusion

During the collision of the side door of the vehicle, the energy absorption of the internal anti-collision bar is poor, which cannot ensure the safety of the personnel in the vehicle. Based on the characteristics of light weight and strong impact resistance of aluminum foam, a foam aluminum composite structure energy absorbing component is designed, which will be combined with the anti-collision pole to improve the energy absorption of the bumper rod. Through the analysis of the mathematical model, simulation results and experimental results of energy absorbing components, the following conclusions are drawn:

1. In static condition, through the analysis of the simulation results and experimental results of the aluminum foam energy absorbing components, it is concluded that the outer diameter of the energy absorbing components increases and the aluminum foam fills up, the greater the peak force is generated. At the same compression displacement, the greater the wall thickness, the greater the corresponding peak force.
2. Under dynamic condition, the filling rate and outer diameter of foam aluminum and the number of energy absorbing components installed in the bumper rod are

taken as independent variables, and the energy absorption characteristics of the energy absorbing components under dynamic collapse are parametrized. At the same time, the higher the filling rate of aluminum foam, the greater the peak force and the more energy absorbed. When the outer diameter of energy absorbing member increases, the compression displacement, specific energy absorption, energy and mass are in an upward trend, and the energy absorption is better; With the increase of wall thickness, the energy absorption index of the energy absorbing component increases, but the slope of the energy absorption curve tends to be gentle. It is proved that the thinner the wall thickness is, the more the foamed aluminum is, the greater the rigid flexible coupling effect between the aluminum foam and the aluminum tube will be. As the number of energy-absorbing components increases, its peak force, energy and mass are increasing. In a certain range, with the increase of the number of energy-absorbing components, the energy absorbing characteristics of the anti-collision bar are obviously enhanced.

3. To meet the optimal energy absorption and the requirements of vehicle lightness. When  $n = 8$ ,  $D = 21$  mm and  $t = 1$  mm, the specific energy absorption value is the largest, which is the optimal solution. In the case of optimal solution, the crashworthiness of optimized rear anti-collision bar and traditional anti-collision bar is compared. The collision load of the anti-collision rod containing aluminum foam composite structure is 126.67kN, and the collision load of the traditional bumper rod is 89.49kN, which is increased by 41.55%. The specific energy absorption of the anti-collision rod containing aluminum foam composite structure is 1035.58 J, the specific energy absorption of the tradi-



tional bumper rod is 690.39 J, the increase is 50.79%, the quality is increased by 17%, and the energy is increased by 80.27%. The mass of the anti-collision bar with energy absorbing components is increased by 17%, but the energy is increased by 80.27%. The added weight is 0.016% of the vehicle weight. Therefore, the filling of the energy absorbing member has certain significance.

In summary, the crashworthiness of the designed anti-collision rod with energy absorbing component aluminum foam composite structure is better than that of the traditional anti-collision rod. It has better effect in energy absorption characteristics and lightweight, and can better meet the development needs of vehicles.

## Declarations

**Conflict of interest** We declare that we have no financial and personal relationships with other people or organizations that can inappropriately influence our work, there is no professional or other personal interest of any nature or kind in any product, service and/or company that could be construed as influencing the position presented in, or the review of, the manuscript entitled.

## References

- Guo C, Mao J, Xie M (2021) Analysis of energy absorption characteristics of corrugated top beams of anti-impact hydraulic supports. *Alex Eng J*. <https://doi.org/10.1016/j.aej.2021.08.077>
- Xi H et al (2021) Energy absorption characteristics of a novel asymmetric and rotatable reentrant honeycomb structure[J]. *Acta Mech Solida Sinica*. <https://doi.org/10.1007/s10338-021-00219-x>
- Anthony G, John M, William A (2021) High capacity, adaptive energy absorption under tensile loading conditions utilizing an axial cutting deformation mode[J]. *Forces Mech* 2:100004. <https://doi.org/10.1016/j.finmec.2020.100004>
- Chen Y, Ye L, Fu K (2021) Progressive failure of CFRP tubes reinforced with composite sandwich panels: Numerical analysis and energy absorption[J]. *Compos Struct*. <https://doi.org/10.1016/j.compstruct.2021.113674>
- Song W et al (2021) Effect of zirconia on low cycle fatigue and energy absorption of molybdenum alloy[J]. *J Alloys Comp*. <https://doi.org/10.1016/j.jallcom.2021.159118>
- Zhang D et al (2019) Energy absorption in the axial crushing of hierarchical circular tubes[J]. *Int J Mech Sci*. <https://doi.org/10.1016/j.ijmecsci.2019.105403>
- Wang Y, Zhang R, Liu S, Zhai X, Zhi X (2021) Energy absorption behaviour of an aluminium foam-filled circular-triangular nested tube energy absorber under impact loading. *Structures*. <https://doi.org/10.1016/j.istruc.2021.07.065>
- Gao Q, Liao WH (2021) Energy absorption of thin walled tube filled with gradient auxetic structures-theory and simulation. *Int J Mech Sci*. <https://doi.org/10.1016/j.ijmecsci.2021.106475>
- Fu J, Liu Q, Ma Y, Zhang Z (2021) A comparative study on energy absorption of flat sides and corner elements in CFRP square tube under axial compression. *Thin-Walled Struct*. <https://doi.org/10.1016/j.tws.2021.108080>
- Feng G, Li S, Xiao L, Song W (2021) Energy absorption performance of honeycombs with curved cell walls under quasi-static compression. *Int J Mech Sci*. <https://doi.org/10.1016/j.ijmecsci.2021.106746>
- Li J, Zhang Y, Kang Y, Zhang F (2021) Characterization of energy absorption for side hierarchical structures under axial and oblique loading conditions. *Thin-Walled Struct*. <https://doi.org/10.1016/j.tws.2021.107999>
- Lu B, Shen C, Zhang J, Zheng D, Zhang T (2021) Study on energy absorption performance of variable thickness CFRP/aluminum hybrid square tubes under axial loading. *Compos Struct*. <https://doi.org/10.1016/j.compstruct.2021.114469>
- Zhao Y, Yang Z, Yu T, Xin D (2021) Mechanical properties and energy absorption capabilities of aluminium foam sandwich structure subjected to low-velocity impact. *Constr Build Mater*. <https://doi.org/10.1016/j.conbuildmat.2020.121996>
- Song W, Xu L, Li N, Zhou Y, Sun T, Li Z, Shen H, Wei S (2021) Effect of zirconia on low cycle fatigue and energy absorption of molybdenum alloy. *J Alloys Comp*. <https://doi.org/10.1016/j.jallcom.2021.159118>
- Praveen Kumar A, Yadi Reddy M, Shunmugasundaram M (2021) Energy absorption analysis of novel double section triangular tubes subjected to axial impact loading. *Mater Today Proc*. <https://doi.org/10.1016/j.matpr.2021.04.485>
- Wang L, Zhang B, Zhang J, Jiang Y, Wang W, Wu G (2021) Deformation and energy absorption properties of cenosphere-aluminum syntactic foam-filled tubes under axial compression. *Thin-Walled Struct*. <https://doi.org/10.1016/j.tws.2020.107364>
- Shan CJ, Li L, Luo J (2013) A liquid analysis of the rectangular wave input signals of hydraulic mufflers[J]. *Appl Mech Mater* 2382:172–176. <https://doi.org/10.4028/www.scientific.net/AMM.312.172>
- Van Dyke C et al (2021) Rapid diagnostic framework for assessing bridge and culvert sensitivity to hydraulic forcing[J]. *Nat Hazad Rev*. [https://doi.org/10.1061/\(ASCE\)NH.1527-6996.0000452](https://doi.org/10.1061/(ASCE)NH.1527-6996.0000452)
- Wu YF, Ge PQ, Bi WB (2021) Analysis of axial force of double circular arc helical gear hydraulic pump and design of its balancing device[J]. *J Cent South Univ* 28(2):418–428. <https://doi.org/10.1007/S11771-021-4612-2>
- Wang H, Su M, Hao H (2021) Compressive properties and energy absorption behavior of Mg17Al12/Al ordered structure composites. *Compos Part B*. <https://doi.org/10.1016/j.compositesb.2021.108688>
- Zhou Y et al (2021) Ballistic response of stitched woven fabrics with superior energy absorption capacity: experimental and numerical investigation. *Compos Struct*. <https://doi.org/10.1016/j.compstruct.2020.113328>
- Partovi A, Shahzamanian MM, Wu PD (2021) Numerical study of mechanical behaviour of tubular structures under dynamic compression. *J Mech Sci Technol* 35:1129–1142. <https://doi.org/10.1007/S12206-021-0226-8>

**Publisher's Note** Springer Nature remains neutral with regard to jurisdictional claims in published maps and institutional affiliations.